ARTIFICIAL SATELLITES, Vol. 55, No 1-2020
DOI: 10.2478/arsa-2020-0002

EFFICIENCY OF USING GNSS-PPP FOR DIGITAL ELEVATION MODEL (DEM) PRODUCTION

Ashraf Abdallah
Department of Civil Engineering, Faculty of Engineering, Aswan University, Aswan, Egypt
e-mail: ashraf.abdallah@aswu.edu.eg

Amgad Saifeldin
Department of Construction and Building Engineering, Arab Academy for Science, Technology and Maritime Transport, Aswan, Egypt
e-mail: eng.amgad@aast.edu

Abdelhamid Abomariam
Department of Civil Engineering, Mattraia, Helwan University, Cairo, Egypt

Reda Ali
Department of Civil Engineering, Mattraia, Helwan University, Cairo, Egypt

ABSTRACT. In the developing countries, cost-effective observation techniques are very important for earthwork estimation, map production, geographic information systems, and hydrographic surveying. One of the most cost-effective techniques is Precise Point Positioning (PPP); it is a Global Navigation Satellite Systems (GNSS) positioning technique to compute precise positions using only a single GNSS receiver. This study aims to evaluate the efficiency of using Global Positioning System (GPS) and GPS/ Globalnaya Navigatsionnaya Sputnikovaya Sistema (GLONASS) post-processed kinematic PPP solution for digital elevation model (DEM) production, which is used in earthwork estimation. For this purpose, a kinematic trajectory has been observed in New Aswan City in an open sky area using dual-frequency GNSS receivers. The results showed that, in case of using GPS/GLONASS PPP solution to estimate volumes, the error in earthwork volume estimation varies between 0.07% and 0.16% according to gridding level. On the other hand, the error in volume estimation from GPS PPP solution varies between 0.40% and 0.99%.

Keywords: Precise point positioning; GNSS; GPS/GLONASS; DEM; CSRS-PPP.

1. INTRODUCTION

Positioning using multiple (Global Navigation Satellite Systems [GNSS]) constellations increases the number of observed satellites, which provide several advantages such as improving accuracy and dilution of precision (DOP) values; moreover, it increases the availability and reliability (Cai and Gao, 2013; Meneghini and Parente, 2017). Nowadays, there are four GNSS operating systems: (1) the American NAVSTAR Global Positioning System (NAVSTAR GPS), (2) the Russian Globalnaya Navigatsionnaya Sputnikovaya

Sistema (GLONASS), (3) the European (Galileo) and (4) the Chinese (BeiDou). However, until 2019, only the GPS and the GLONASS are fully operated.

Owing to the large errors of the broadcast ephemeris, including satellite orbit and clock, as well as atmospheric effect, the delivered accuracy for absolute positioning could not be better than a few meters. To get a centimetre positioning accuracy level, one option is called relative positioning or differential Global Navigation Satellite Systems (DGNSS). DGNSS is a method of improving the positioning accuracy that uses a fixed known position ground reference station (base station). The second GNSS receiver, which is called the rover, can be in static or kinematic mode. Both receivers need to observe simultaneously the same satellites. The errors affecting the observations of base and rover are very similar: so the baseline between base and rover can be estimated accurately (Hoffmann-Wellenhof et al., 2008).

However, DGNSS has three main defects: (1) the necessity to establish a known base receiver station, (2) the necessity for simultaneous observations at the base and rover receiver stations and (3) the degradation of accuracy with the increasing distance between the base station and rover receiver (Rizos et al., 2012). Therefore, Precise Point Positioning (PPP) processing approach, which does not need a base station, is an efficient alternative to DGNSS methods. The concept of PPP was developed with the advent of GNSS products, including precise orbit, satellite clock, phase centre offset for satellite and receiver and atmospheric corrections.

Since the first effective PPP model was processed by Zumberge et al. (1997), a lot of PPP processing software packages have been developed, especially for dual-frequency PPP (e.g. gLAB (Sanz et al., 2012) and GAMP (Zhou et al., 2018)), and Bernese GNSS software V. 5.2 (Dach et al., 2007). Moreover, many free PPP online services are available; for example, Canadian Spatial Reference System (CSRS) (CSRS-PPP, 2019), Automatic Precise Point Service (APPS-PPP), GPS Analysis and Positioning Software (GAPS-PPP, 2019) and magicGNSS solution (magicGNSS, 2019).

The research to date has tended to focus on investigating the accuracy of the combined GPS/GLONASS PPP model. Cai and Gao (2013) presented a combined GPS/GLONASS PPP model for a vehicle trajectory. They reported that the combined GPS and GLONASS PPP solution can provide a root mean square error (RMSE) of 8.3, 4.3 and 18.3 cm in east, north and height components, respectively. These results improved positioning accuracy by 57%, 69% and 65% in east, north and height, respectively, over GPS only. According to Alkan et al. (2017), processed, combined GPS and GLONASS kinematic data were collected in the marine environment using CSRS-PPP online service and compared with DGNSS. The research found that adding GLONASS data to GPS data did not significantly improve the positioning accuracy. The results of mean error are 6 cm for the horizontal position and 10 cm in height. Farah (2018) evaluated the accuracy for dual- and single-frequency kinematic PPP for hydrography. The delivered average accuracy using GPS constellation was <2 cm for horizontal and 5 cm for height. In the other direction, adding GLONASS satellites improved the accuracy by 26%.

2. COMBINED GPS AND GLONASS PPP MODEL

For two decades, the most effective PPP estimation model has been introduced by the researching group of the Jet Propulsion Laboratory (JPL) (Zumberge et al., 1997). To deliver a centimetre accuracy level of PPP model, four types of corrections are modelled or eliminated: (1) satellite-dependent errors are included in the satellite clock and orbit data; moreover, satellite antenna phase centre and phase wind-up errors. (2) Receiver-dependent errors include receiver antenna phase centre and antenna phase wind-up errors. (3) Atmospheric errors consist of tropospheric and ionospheric delay. Finally, (4) geophysical

errors cover solid earth tides, polar tides, ocean tide loading, earth rotation and atmospheric tidal loading (Rizos et al., 2012). Table (1) illustrated the effects of different errors on positions.

Table 1. PPP corrections effects of positions after (Rizos et al., 2012), and (Abdallah, 2016)

Error	Correction	Impact on position
Ephemerides	Correction of satellite coordinates	2.1 m (Hoffmann-Wellenhof et al., 2008)
Satellite clocks	Correction of satellite clocks	2.1 m (Hoffmann-Wellenhof et al., 2008)
Satellite antenna offset	Correction of satellite coordinates	height: up to 10 cm position: several cm
Satellite phase variation	Correction of carrier-phase observation	height: several mm
Satellite phase wind-up effect		
Ionosphere delay	Correction of station coordinates	1–15 m for mid-latitude Reach 36 m near equatorial (Mirsa and Enge, 2012)
Troposphere delay		2.30–2.60 m at sea level (Mirsa and Enge, 2012)
Solid earth tides (site displacement Effect)	Correction of station coordinates	height: several decimetre (dm) position: several centimetre
Ocean tide loading (site displacement effect)	Correction of stations near the coasts	height: up to 5 cm
Earth rotation parameters (ERP site displacement effect)	Correction of station coordinates used)	height: several centimetre position: several centimetre
Atmospheric loading	Correction of atmospheric pressure loading	Height: up to 18 mm for 24-hour observation data (Tregoning and van Dam, 2005)

The observed code pseudo-range (ρ) in metres is modelled by considering the previous errors in equation (1), as well as the phase pseudo-range ($\lambda\Phi$) in metres is modelled by considering the previous errors in equation (2) (Abdallah, 2016), where the superscript S refers to GNSS satellite and the subscript R refers to GNSS receiver.

$$\rho = r + c(\delta^R - \delta^S) + \Delta_{iono} + \Delta_{trop} + \Delta_{sol} + \Delta_{pol} + \Delta_{ocn} + \Delta_{atm} + \Delta_{mul} + \in_{\rho} \quad (1)$$

$$\lambda\Phi = r + c(\delta^R - \delta^S) - \Delta_{iono} + \Delta_{trop} + \lambda N + \Delta_{sol} + \Delta_{pol} + \Delta_{ocn} + \Delta_{atm} + \Delta_{mul} + \Delta_{pcv} + \lambda w + \in_{\Phi} \quad (2)$$

The PPP model is mainly based on eliminating the ionospheric delay by combining the dual-frequency measurements that call the ionospheric-free linear combination for code ($\rho^S_{R\,IF}$), and carrier phase ($\Phi^S_{R\,IF}$). The higher-order ionospheric terms are recommended to be removed for more accurate applications according to Keder et al. (2003), and Bassiri and Hajj (1993). The tropospheric delay consists of two parts: the dry part that represent 90% of total delay and the wet part that is difficult to model due to the high variation of water vapour in respect to time (Hoffmann-Wellenhof et al., 2008). By considering the arbitrary zenith angle of GPS signal, the tropospheric delay is modelled with relating to the elevation angle of observed satellites. Therefore, a mapping function is the simplified form for dry and wet

tropospheric delay (Mirsa and Enge, 2012). This combination is given in equations (3) and (4) (Mirsa and Enge, 2012).

$$\rho^{S}_{R\,IF} = \frac{f_{l1}^2\,\rho_{l1} - f_{l2}^2\,\rho_{l2}}{(f_{l1}^2 - f_{l2}^2)} = 2.546\rho_{l1} - 1.546\rho_{l2} \quad (3)$$

$$\Phi^{S}_{R\,IF} = \frac{f_{l1}^2\,\Phi_{l1} - f_{l2}^2\,\Phi_{l2}}{(f_{l1}^2 - f_{l2}^2)} = 2.546\Phi_{l1} - 1.546\Phi_{l2} \quad (4)$$

Δ_{iono} is the ionospheric delay,
Δ_{trop} is the tropospheric delay,
Δ_{sol} is the solid earth tides error,
Δ_{pol} is the pole tides error,
Δ_{ocn} is the ocean loading effect,
Δ_{atm} is the atmospheric loading effect,
Δ_{mul} is the multipath effect,
Δ_{pcv} is the antenna phase centre variation,
w is the correction of phase wind-up,
δ^{R} is the receiver clock bias,
δ^{S} is the satellite clock bias,
c is the speed of light,
r is the true range between receiver (x_R, y_R, z_R) and satellite (x_S, y_S, z_S) coordinates,
λ is the carrier wave length,
N is the ambiguity integer,
$\rho^{S}_{R\,IF}$ is the ionosphere-free combination of code ranges,
$\Phi^{S}_{R\,IF}$ is the ionosphere-free combination of carrier phases,
f_{L1}, f_{L2} are the GNSS frequencies of L_1 and L_2 signals,
ρ_{l1}, ρ_{l2} are the code range of L_1 and L_2 signals,
Φ_{L1}, Φ_{L2} are the carrier phase of L_1 and L_2 signals,
$\in_{\rho}$ and $\in_{\Phi}$ are the relevant measurement noises.

3. SECTION WITH SUBSECTIONS

To identify the PPP solution, a kinematic trajectory (layout is illustrated in Figure 1) has been observed on 27 July 2018 in New Aswan City using a GNSS receiver of Topcon HiPer Ga. The observation duration of the kinematic trajectory was 1 h and 10 min with a sampling interval of 5 s. The GNSS antenna was set up on a backpack to perform the kinematic measurements (see Figure 2). To assess the efficiency of using PPP technique in DEM production, a parcel of land with an area of 8 acres was chosen to conduct the experiment (see Figure 1); the land boundary is marked by blue solid line, and the kinematic walking trajectory is marked by red dots.

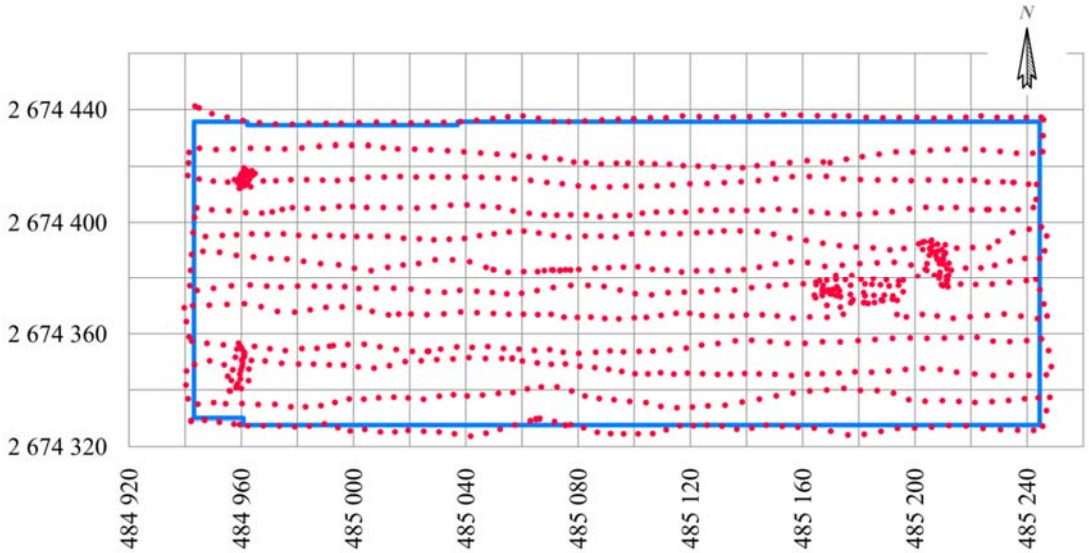

Figure 1. Layout of walking trajectory used for DEM production, coordinates (WGS84/UTM zone 36N) and units in metre.

Figure 2. Base and rover GNSS receivers.

To evaluate the performance of kinematic PPP solution for GPS only and GPS/GLONASS, the projected coordinates (WGS84/UTM zone 36N) were obtained from CSRS-PPP. The CSRS-PPP is a popular free online processing service offered from the natural resources of Canada to provide a PPP solution for GNSS observation data (Krasuski, 2015). This service is capable of processing code and phase observations; it processes single or dual frequency for static or kinematic. Table 2 summarizes the processing parameters of CSRS-PPP software. The reference system for the software is based on International Terrestrial Reference Frame (ITRF) 2014; the estimated coordinates are in format Cartesians XYZ format and as well in ellipsoidal/ Universal Transverse Mercator (UTM) system.

The International GNSS Service (IGS) final ephemerides are used during the processing with a satellite orbit of 15-min interval and clock of 30-s interval. The ionospheric delay is basically modelled using the ionospheric free linear combination; moreover, the second-order errors are considered, as well. With regard to the tropospheric delay, the software uses Davis model for the hydrostatic delay, which is based on the global pressure and temperature (GPT)

model. For wet part, the software is used the Hopfield model, which is based on the GPT model; furthermore, global mapping function is used. For the satellite and receiver, antenna phase variations are based on IGS-ANTEX format (NGS, 2019; CSRS-PPP, 2018).

Table 2. Processing parameters

ID	Processing parameter
Reference system	ITRF2014
Coordinate format	XYZ/ellipsoidal/UTM
Ephemerides	IGS final (orbit: 15-min interval and clock: 30-s interval)
Phase centre offsets	IGS ANTEX
Ionospheric model	Linear ionospheric free combination + second-order parameters
Tropospheric model	Dry: Davis (GPT) Wet: Hopfield model (GPT) GMF

For processing procedure, the kinematic PPP solution for GPS only and combined GPS/GLONASS for each epoch are compared using post-processed differential kinematic GNSS solution, which is considered as a reference solution. The DGNSS solution was obtained using Leica Geo Office 7 software; the static data collected from a reference station were processed with the kinematic data collected by the GNSS receiver located over the backpack. As shown in Figure 3, the GNSS data for base and rover receivers have been checked for the quality using TEQC software.

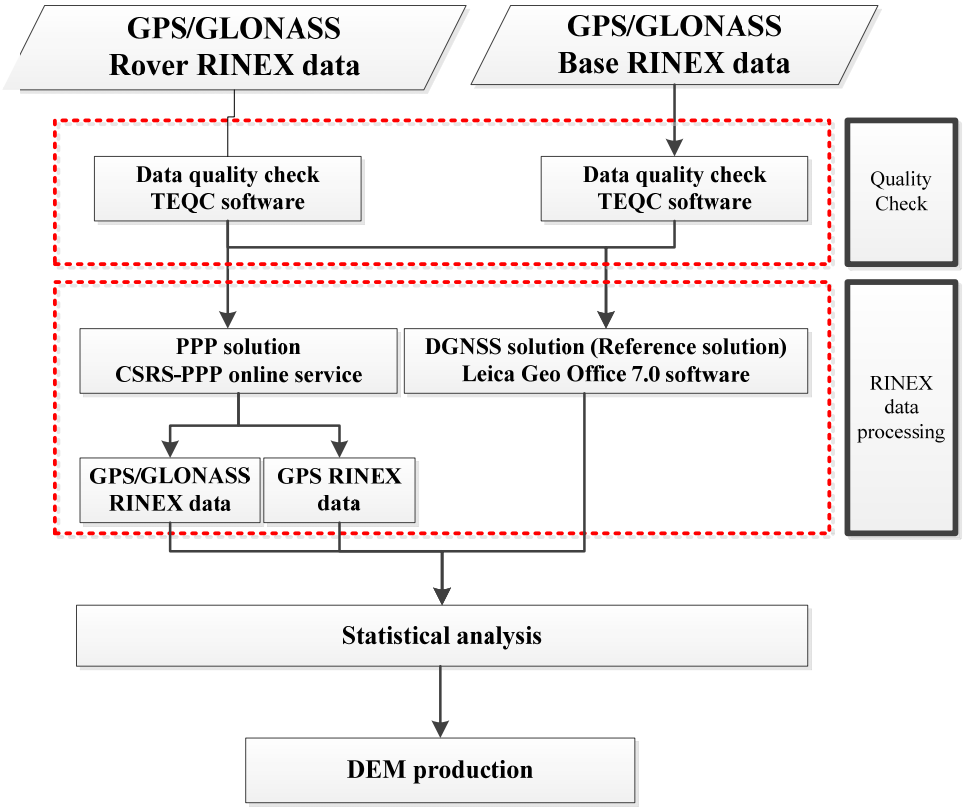

Figure 3. Processing procedure.

4. RESULTS AND ANALYSIS

In order to estimate the accuracy of kinematic PPP solution, the positioning errors in horizontal position and height of GPS and GPS/GLONASS PPP solutions are shown in Figure 4. For horizontal direction, there were no significant difference between GPS and GPS and GPS/GLONASS observations. For height direction, a significant improvement has been obtained using GPS/GLONASS observation. Adding of GLONASS observations to GPS observations significantly improved the height positioning accuracy. Figure 5 provides the number of satellites and Geometric Dilution of Precision GDOP for GPS and GPS/GLONASS; the average number of satellites for GPS only is 8 and that for combined GPS and GLONASS is 14. The addition of GLONASS observations to GPS observations improved GDOP value by 12.7%.

For more statistical analysis, Table 3 illustrates the minimum and maximum errors in horizontal position and height for GPS and GPS/GLONASS (see Figure 6). The Root Mean Square RMS errors for the GPS PPP solution compared with DGNSS solution show 2.9 cm for horizontal position and 3.2 cm for height. The RMS errors for the GPS/GLONASS PPP solution show 2.9 cm for horizontal position and 1.8 cm for height. The kinematic GPS/GLONASS PPP solution improved height accuracy by 43.8% over the GPS PPP. On the other hand, GPS/GLONASS PPP solution did not improve horizontal position accuracy. For GPS and GPS/GLONASS PPP solutions, the RMSE in horizontal position did not exceed 2.9 cm and the RMSE in height did not exceed 3.2 cm, which meets the accuracy requirements for topographic maps at a scale of 1:200 with a contour interval of 10 cm (Federal Geographic Data Committee, 1998).

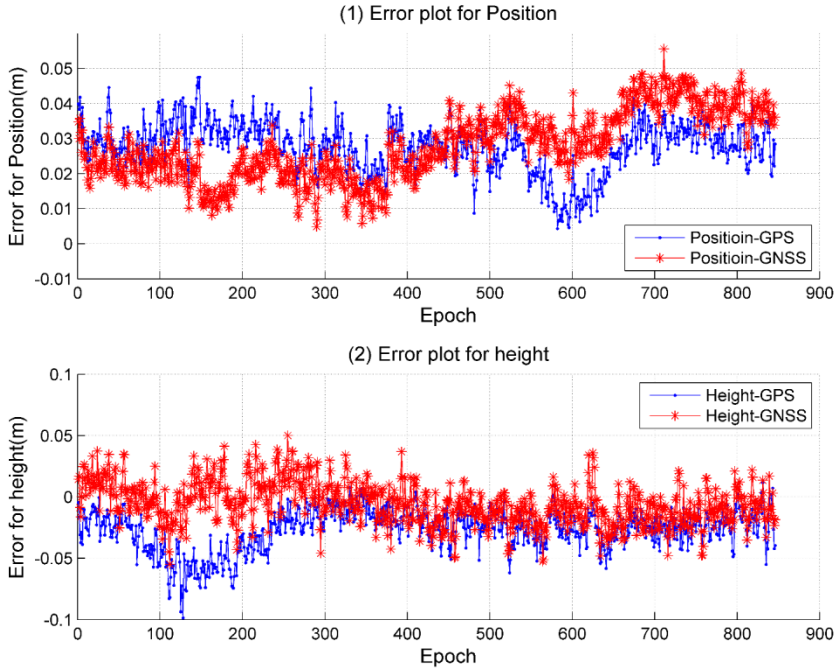

Figure 4. Kinematic PPP errors in horizontal position and height (cm) for GPS and GPS/GLONASS.

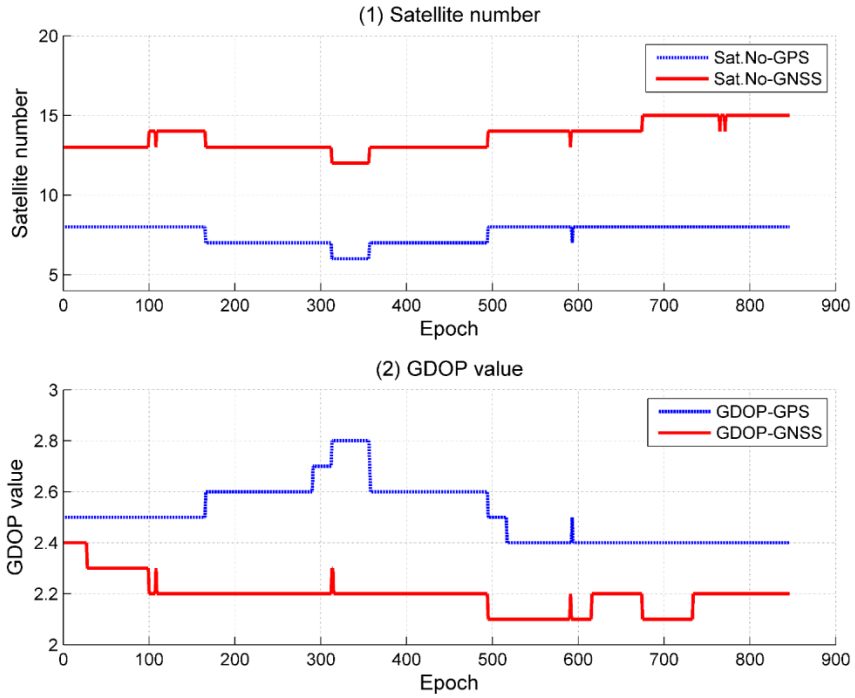

Figure 5. Satellite number and GDOP value.

Table 3. Statistical analysis of the kinematic PPP solution.

	Error in horizontal position (cm)			Error in height (cm)		
	Min	**Max**	**RMSE**	**Min**	**Max**	**RMSE**
GPS only	0.4	4.8	2.9	−1.2	9.9	3.2
GPS/GLONASS	0.5	5.6	2.9	−5	5.5	1.8

5. DIGITAL ELEVATION MODEL PRODUCTION

DEM is a digital representation of ground surface (Mukherjee et al., 2012). DEM can be used in many applications, such as site and route selection, geomorphology, hydraulic modelling and mapping (Peckham and Gyozo, 2007; Bangen et al., 2014; Bolkas et al., 2016). There are different techniques to produce DEM, such as field surveying using total station, DGNSS and terrestrial laser scanner, aerial photogrammetry, airborne light detection and ranging (LiDAR) and radar interferometry (Patel, Katiyar and Prasad, 2016).

The DEMs produced by DGNSS, GPS/GLONASS PPP and GPS PPP are showed in Figure 7, which illustrates that the DEM produced by DGNSS and that produced by GPS/GLONASS PPP are approximately identical. On the other hand, the DEM produced by GPS PPP is slightly different from the other two DEMs.

Earthwork volume estimation is very important for various civil engineering projects such as building construction, highway construction, and irrigation projects. To evaluate the efficiency of PPP kinematic solution for DEM production, the volume between the surface produced by DGNSS and the surface produced by GPS/GLONASS PPP were calculated using Civil 3D software. The cut volume is equal to 280 m^3, and the fill volume is equal to 127 m^3. The error in volume estimation (net cut volume/total area) is 19.125 m^3/acre (this shows an error of ±0.47 cm over the total area). On the other hand, the error in net cut volume in case of GPS PPP is 114.25 m^3/acre.

For more statistical data, Table 4 provides the volume of cut and fill for three different scenarios. In the first scenario, the area is levelled to the lowest elevation (149.00 m); the error percentage for cut volume calculation is 0.07% for GPS/GLONASS PPP and 0.40% for GPS PPP. In case of the second scenario, the area is levelled to the highest elevation (162.00 m); the error percentage for fill volume calculation is 0.08% for GPS/GLONASS PPP and 0.48% for GPS PPP. In the third scenario, the area is levelled to elevation 156.06 m, which gives approximately equal cut and fill volume; the error percentage for cut volume calculation is 0.16% for GPS/GLONASS PPP and 0.99% for GPS PPP, and the error percentage for fill volume calculation is 0.12% for GPS/GLONASS PPP and 0.73% for GPS PPP.

Table 4. Cut and fill volume from DEMs produced by three different techniques.

	Grading to level 149		**Grading to level 162**		**Grading to level 156.06**	
	Cut m^3	Fill m^3	Cut m^3	Fill m^3	Cut m^3	Fill m^3
DGNSS	228,763	0	0	192,249	53,351	53,229
GPS + GLONASS	228,917	0	0	192,095	53,438	53,163
GPS only	229,677	0	0	191,334	53,879	52,843

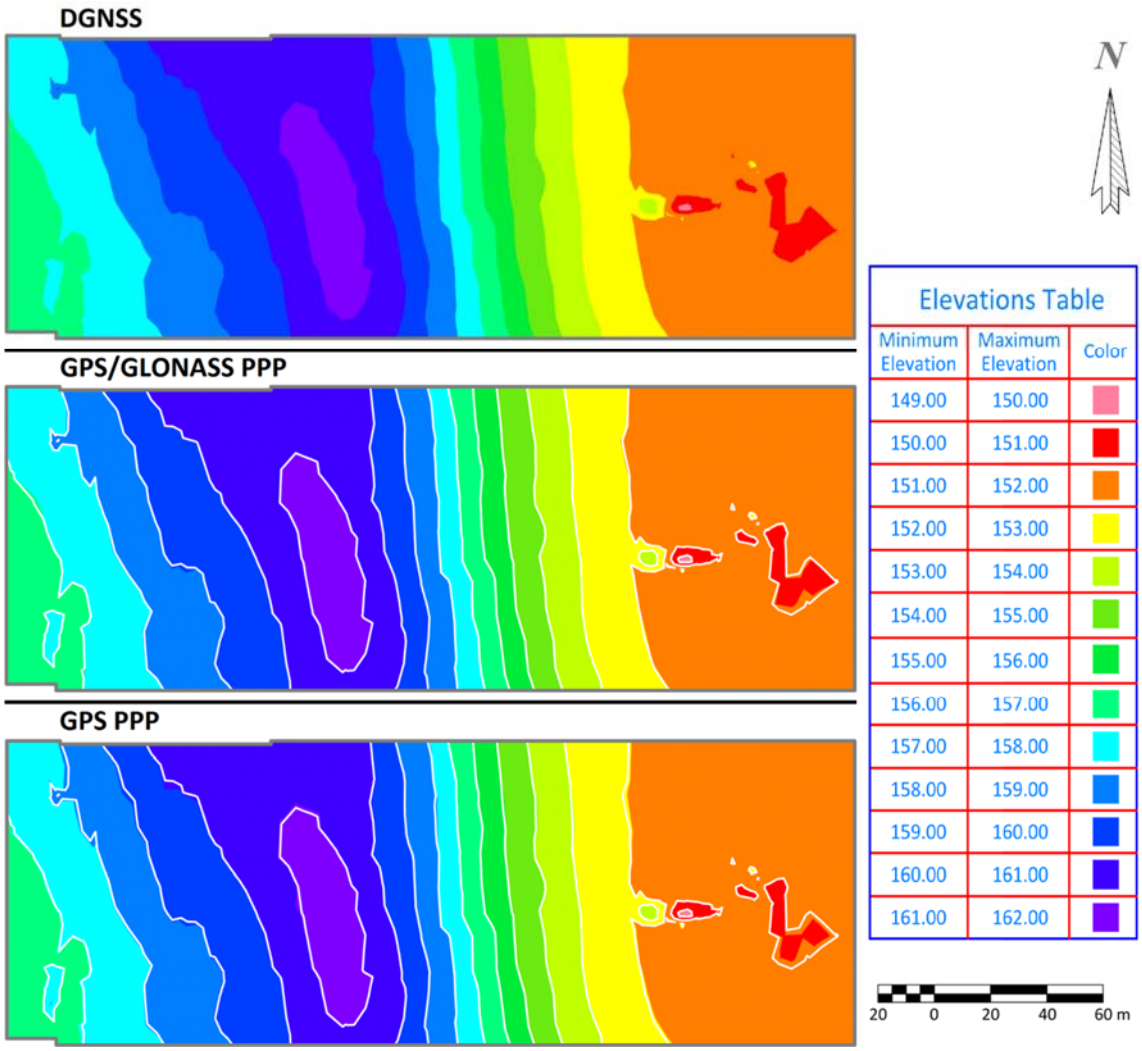

Figure 6. DEMs produced by DGNSS, GPS/GLONASS PPP and GPS PPP.

6. CONCLUSIONS

In this study, the performance of kinematic PPP using GPS only and combined GPS/GLONASS was evaluated through observation of kinematic trajectory in New Aswan City, Egypt. The kinematic PPP solution was obtained by CSRS-PPP online service. The PPP solution was compared to DGNSS as a reference solution. The experiment was conducted on 27 July 2018 over 8-acres area. The kinematic trajectory was observed for 1 h and 10 min. The numerical results showed that the RMS errors for the GPS-only PPP solution are 2.9 cm for horizontal position and 3.2 cm for height. The RMS errors for the combined GPS and GLONASS PPP solution are 2.9 cm for horizontal position and 1.8 cm for height.

Furthermore, this research investigates the efficiency of using GPS PPP and GPS/GLONASS PPP to produce DEM through estimating earthwork volumes under three different scenarios. The first one is gridding the area to the lowest level (149 m); in the second scenario, the area was gridded to the highest elevation (162.00 m); and in the last case, the area was levelled to intermediate elevation (156.06 m) that gives approximately equal cut and fill volume. The error in volume estimation varies between 0.07% and 0.16% for DEM produced by GPS/GLONASS PPP. On the other hand, the DEM produced by GPS PPP has an error between 0.40% and 0.99%. From results, it can be concluded that, first, the addition of GLONASS observations to GPS observations improves height accuracy significantly; second, PPP using online GNSS processing services is accurate and low-cost positioning technique for DEM production.

Acknowledgements. The authors would like to thank the consulting office of El-Massa Consult (M.Sc. Eng. Nahla Abdelkader) for providing the authors with the GNSS instruments (Topcon Hipper Ga) and funding the experimental work.

REFERENCES

Alkan, R. M., Saka, M. H., Ozulu, M. and İlçi, V. (2017) 'Kinematic precise point positioning using GPS and GLONASS measurements in marine environments', Measurement: Journal of the International Measurement Confederation, 109, pp. 36–43. doi: 10.1016/j.measurement.2017.05.054.

Bangen, S. G., Wheaton, J. M., Bouwes, N., Bouwes, B. and Jordan, C. (2014) 'A methodological intercomparison of topographic survey techniques for characterizing wadeable streams and rivers', Geomorphology, 206, pp. 343–361. doi: 10.1016/j.geomorph.2013.10.010.

Bolkas, D., Fotopoulos, G., Braun, A. and Tziavos, I. N. (2016) 'Assessing Digital Elevation Model Uncertainty Using GPS Survey Data', Journal of Surveying Engineering, 142(3), pp. 1–8. doi: 10.1061/(ASCE)SU.1943-5428.0000169.

Cai, C. and Gao, Y. (2013) 'Modeling and assessment of combined GPS/GLONASS precise point positioning', GPS Solutions, 17(2), pp. 223–236. doi: 10.1007/s10291-012-0273-9.

Farah, A. (2018) 'Kinematic-PPP using Single/Dual Frequency Observations from (GPS, GLONASS and GPS/GLONASS) Constellations for Hydrography' Artificial Satellites 53(1): 37-46.

Federal Geographic Data Committee (1998) Geospatial Positioning Accuracy Standards Part 3 : National Standard for Spatial Data Accuracy, National Spatial Data Infrastructure. Reston, Virginia. doi: FGDC-STD-007.3-1998.

Hofmann-Wellenhof, B., Lichtenegger, H. and Wasle, E. (2008) GNSS — Global Navigation Satellite Systems. 1st edn. Springer-Verlag Wien. doi: 10.1007/978-3-211-73017-1.

Meneghini, C. and Parente, C. (2017) 'Advantages of Multi GNSS Constellation: GDOP Analysis for GPS, GLONASS and Galileo Combinations', International Journal of Engineering and Technology Innovation; Vol 7, No 1 (2017). Available at: http://ojs.imeti.org/index.php/IJETI/article/view/367 .

Mukherjee, S., Joshi, P. K., Mukherjee, S., Ghosh, A., Garg, R. D. and Mukhopadhyay, A. (2012) 'Evaluation of vertical accuracy of open source Digital Elevation Model (DEM)', International Journal of Applied Earth Observation and Geoinformation. Elsevier B.V., 21(1), pp. 205–217. doi: 10.1016/j.jag.2012.09.004.

Patel, A., Katiyar, S. K. and Prasad, V. (2016) 'Performances evaluation of different open source DEM using Differential Global Positioning System (DGPS)', Egyptian Journal of Remote Sensing and Space Science. Authority for Remote Sensing and Space Sciences, 19(1), pp. 7–16. doi: 10.1016/j.ejrs.2015.12.004.

Peckham, R. and Gyozo, J. (2007) Digital terrain modelling: development and applications in a policy support environment. 1st edn. Springer-Verlag Berlin Heidelberg. doi: 10.1007/978-3-540-36731-4.

Rizos, C., Janssen, V., Roberts, C. and Grinter, T. (2012) 'Precise Point Positioning: Is the Era of Differential GNSS Positioning Drawing to an End?', in FIG Working Week 2012, pp. 1–17. Available at: https://eprints.utas.edu.au/13280/ .

Sanz, J., Rovira-Garcia, A., Hernández-Pajares, M., Juan, M., Ventura-Traveset, J., López-Echazarreta, C. and Hein, G. (2012) 'The ESA/UPC GNSS-Lab Tool (gLAB): an advanced educational and professional package for GNSS data processing and analysis', in 6th ESA Workshop on Satellite Navigation Technologies Multi-GNSS Navigation Technologies. Noordwijk, the Netherlands.

Teunissen, P. J. G. and Montenbruck, O. (2017) Springer handbook of global navigation satellite systems. 1st edn. Springer International Publishing. doi: 10.1007/978-3-319-42928-1.

Zhou, F., Dong, D., Li, W., Jiang, X., Wickert, J. and Schuh, H. (2018) 'GAMP: An open-source software of multi-GNSS precise point positioning using undifferenced and uncombined observations', GPS Solutions, 22(2), p. 33. doi: 10.1007/s10291-018-0699-9.

Zumberge, J. F., Heftin, M. B., Jefferson, D., Watkins, M. M. and Webb, F. H. (1997) 'Precise point positioning for the efficient and robust analysis of GPS data from large networks', Journal of Geophysical Research, 102(10), pp. 5005–5017. doi: 10.1029/96JB03860.

Websites:

GAPS-PPP (2019): GNSS Analysis and Positioning Software, ©University of New Brunswick, Available at: http://gaps.gge.unb.ca/, Access on 19th July, 2019.

APPS-PPP (2019): Automatic Precise Positioning Service, Jet Propulsion Laboratory, California Institute of Technology. Available at: http://apps.gdgps.net/, Access on 19th July, 2019.

CSRS-PPP (2019): The Canadian Spatial Reference System (CSRS) Precise Point Positioning (PPP). Available at: https://webapp.geod.nrcan.gc.ca/geod/tools-outils/ppp.php, Access on 19th July, 2019.

magicGNSS (2019): magicGNSS web service, Available at: https://magicgnss.gmv.com/, Access on 19th July, 2019.

Received: *2019-09-23*

Reviewed: *2019-10-07 (by K. Krasuski), 2019-10-16 (by A. Łyszkowicz) and 2019-11-13 (by B. Oszczak)*

Accepted: *2020-03-17*